Nanotechnology

Catalytic Growth of Au Nanoparticles by NAD(P)H Cofactors: Optical Sensors for NAD(P)$^+$-Dependent Biocatalyzed Transformations**

*Yi Xiao, Valeri Pavlov, Semion Levine, Tamara Niazov, Gil Markovitch, and Itamar Willner**

Increasing efforts are directed to the application of metal and semiconductor nanoparticles (NPs) for the development of electronic or optical sensory systems.[1] Metal or semiconductor NPs functionalized with nucleic acids were employed as amplifying labels for the detection of DNA; the dissolution of the nanoparticles was used to follow DNA hybridization events.[2] Also, charge injection from semiconductor nanoparticles into electrodes and the generation of photocurrents was used to follow hybridization processes[3] and biocatalytic transformations.[4] The catalytic deposition of metals onto metal nanoparticles conjugated to DNA-hybridized complexes on surfaces was used as a sensor for DNA through conductivity[5] or microgravimetric quartz crystal microbalance[6] measurements.

The optical detection of processes in the presence of metal and semiconductor NPs has become a common practice in analysis. Besides the use of semiconductor quantum dots as fluorescence labels in sensors,[7] the fluorescence quenching of semiconductor quantum dots has been employed in different sensing paths.[8] The plasmon absorbance of metal nanoparticles, such as Au NPs, and specifically the interparticle-coupled plasmon absorbance of aggregated NPs was extensively used to follow molecular[9] and biomolecular[10] recognition processes. The use of semiconductor or metallic NPs as probes to follow biocatalytic processes is less established, with only a few reports for these applications.[4,11] Nicotinamide adenine dinucleotide (NAD^+)- and nicotinamide adenine dinucleotide phosphate ($NADP^+$)-dependent enzymes are important in biocatalyzed synthesis.[12] Extensive efforts have been directed towards the development of electrochemical sensors based on NAD(P)$^+$-dependent enzymes.[13] Herein, we report the catalyzed growth of gold nanoparticles in the presence of NAD(P)H cofactors. We apply the process to the quantitative optical analysis of NAD(P)H cofactors and to the analysis of NAD(P)$^+$-dependent biocatalyzed reactions in solutions and on surfaces.

[*] Dr. Y. Xiao, Dr. V. Pavlov, S. Levine,[+] T. Niazov, Prof. I. Willner
Institute of Chemistry, The Hebrew University of Jerusalem
Jerusalem 91904 (Israel)
Fax: (+972) 2-652-7715
E-mail: willnea@vms.huji.ac.il
Dr. G. Markovitch
School of Chemistry, Tel-Aviv University
Tel-Aviv 69978 (Israel)
[+] Deceased, April 14, 2004

[**] This research was supported by the Israel Ministry of Commerce and Industry as part of a Nofar project.

The solution for the growth of the particles consisted of citrate-stabilized Au NPs (4.0×10^{-10} M in 13 nm ± 1-nm particles), $HAuCl_4$ (1.8×10^{-4} M), and CTAB (7.4×10^{-2} M) as a surfactant. Figure 1 shows the changes in the UV/Vis spectra

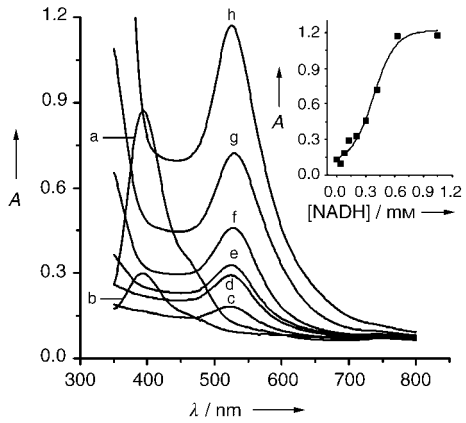

Figure 1. Variation in the absorbance spectra of the Au NP growth solution (4.0×10^{-10} M in Au NPs) at different concentrations of NADH: a) 0 M; b) 4.2×10^{-5} M; c) 8.4×10^{-5} M; d) 12.6×10^{-5} M; e) 21×10^{-5} M; f) 30×10^{-5} M; g) 42×10^{-5} M; h) 63×10^{-5} M. Inset: Variation in the absorbance intensity at $\lambda = 524$ nm of the growth solution upon interaction (30 mins) with variable concentrations of NADH.

of the growth solution upon interaction with different concentrations of NADH. In the absence of NADH, the solution displays an absorbance band at $\lambda = 392$ nm, characteristic of the $AuCl_4^-$ component (Figure 1, curve a). Upon addition of NADH, this band disappears instantaneously and the characteristic orange color of the system is depleted (curve b), and then the slow buildup of the absorbance of the particle plasmon is observed. As the concentration of NADH increases, the absorbance of the Au particles increases and is shifted to longer wavelengths (from 523 to 530 nm; Figure 1, curves c–h). The inset in Figure 1 shows the calibration curve derived from the changes in the absorbance at $\lambda = 524$ nm as the concentration of NADH increases.

Figure 2 shows the changes in the absorbance of the Au NP growth solution upon interaction with different concentrations of the NADPH cofactor. The absorbance of the Au particles increases and is shifted to longer wavelengths as the concentration of the reduced cofactor is increased. Figure 2 inset, shows the calibration curve that corresponds to the absorbance of the Au particles at $\lambda = 524$ nm at different concentrations of NADPH. Control experiments reveal that all of the components of the growth solution are essential for the enhanced growth of the Au particles. Exclusion of the Au NPs from the solution does not yield any gold particles upon the addition of the NAD(P)H cofactors which implies that although the $AuCl_4^-$ salt is reduced to the colorless Au^I species by the NAD(P)H cofactors, the Au NP seeds are required as catalysts for the growth of the particles. The surfactant CTAB is also essential to stimulate the growth of the Au NPs upon the addition of NAD(P)H. Clearly, the enlargement of the Au NP seeds by the NAD(P)H/$AuCl_4^-$ solutions involves two steps: First, the rapid reduction of

 DOI: 10.1002/ange.200460608

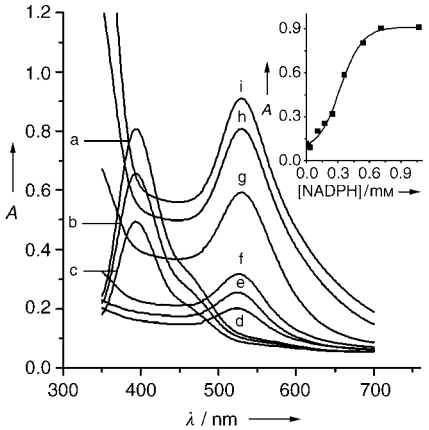

Figure 2. Variation in the absorbance spectra of the Au NP growth solution (4.0×10^{-10} M in Au NPs) at different concentrations of NADPH: a) 0 M; b) 1.79×10^{-5} M; c) 3.57×10^{-5} M; d) 10.7×10^{-5} M; e) 18×10^{-5} M; f) 25×10^{-5} M; g) 36×10^{-5} M; h) 54×10^{-5} M; i) 71×10^{-5} M. Inset: Variation in the absorbance intensity at $\lambda = 524$ nm of the growth solution upon interaction (30 mins) with variable concentrations of NADPH.

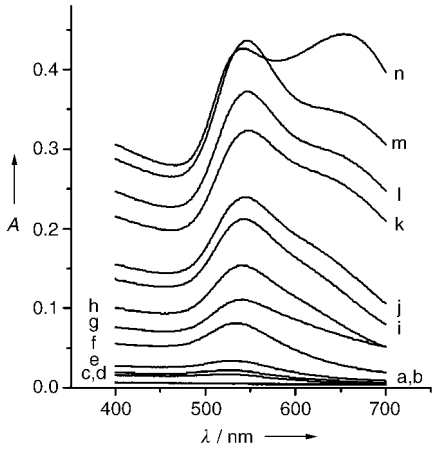

Figure 3. Changes in the absorbance of the Au NP/aminopropylsiloxane-functionalized glass slides upon treatment with the growth solution in the presence of different concentrations of NADH: a) 0 M; b) 14×10^{-5} M; c) 27×10^{-5} M; d) 34×10^{-5} M; e) 41×10^{-5} M; f) 44×10^{-5} M; g) 48×10^{-5} M; h) 51×10^{-5} M; i) 54×10^{-5} M; j) 58×10^{-5} M; k) 61×10^{-5} M; l) 65×10^{-5} M; m) 68×10^{-5} M; n) 1.36×10^{-3} M.

$AuCl_4^-$ by NAD(P)H to the colorless Au^I species takes place as described in Equation (1) (this result is similar to earlier reports[14] in which other reducing agents were employed). Second, the slow catalyzed reduction of the Au^I species by the Au NP seeds to the Au metal particles occurs, [Eq. (2)].

$$AuCl_4^- + NADH \rightarrow Au^I + 4\,Cl^- + NAD^+ + H^+ \quad (1)$$

$$2\,Au^I + NADH \xrightarrow{\text{Au-NP}} 2\,Au^0 + NAD^+ + H^+ \quad (2)$$

The growth of the Au NPs by the NAD(P)H cofactors was also examined on surfaces. Glass slides were functionalized with a 3-aminopropylsiloxane film, and the citrate-stabilized Au-NPs (3 nm ± 1 nm, prepared by reduction with $NaBH_4$ and further stabilized by citrate) were electrostatically bound to the surface.[15] The resulting Au nanoparticle-functionalized glass slides were then treated with the growth solution and different concentrations of the NADH cofactor. Figure 3 depicts the changes in the absorbance spectra of the glass interfaces upon interaction with different concentrations of NADH. Visually, the color of the glass slides turns from red to dark blue depending on the concentration of NADH in solution. As the concentration of NADH is increased, the absorbance spectra of the surfaces reveal an increase in the absorbance band at $\lambda = 535$ nm. At NADH concentrations that are higher than 0.55 mM, the evolution of a second absorbance band at $\lambda = 650$ nm is observed. This absorbance was previously attributed to an interparticle-coupled plasmon exciton that forms upon the aggregation and intimate contact of the Au particles.[16] Thus, at high concentrations of NADH, the growth of the Au NPs on the surface brings the Au particle aggregates into close contact to give rise to the long-wavelength absorbance band.

To understand further the growth mechanism of the Au NP seeds by the $AuCl_4^-$/NADH system, we analyzed the Au NP-functionalized glass surfaces with scanning electron microscopy (SEM). Upon increasing the concentration of NADH from 6.8×10^{-5} to 27×10^{-5} to 41×10^{-5} to 54×10^{-5} M (Figures 4 a–d, respectively), the surface coverage of the enlarged Au particles on the glass surfaces also increases, with the particles exhibiting dimensions of 6 ± 1, 13 ± 2, 18 ± 5, and 40 ± 8 nm, respectively. The SEM images in Figures 4 a–d show isolated, noncontacted particles whose behavior is

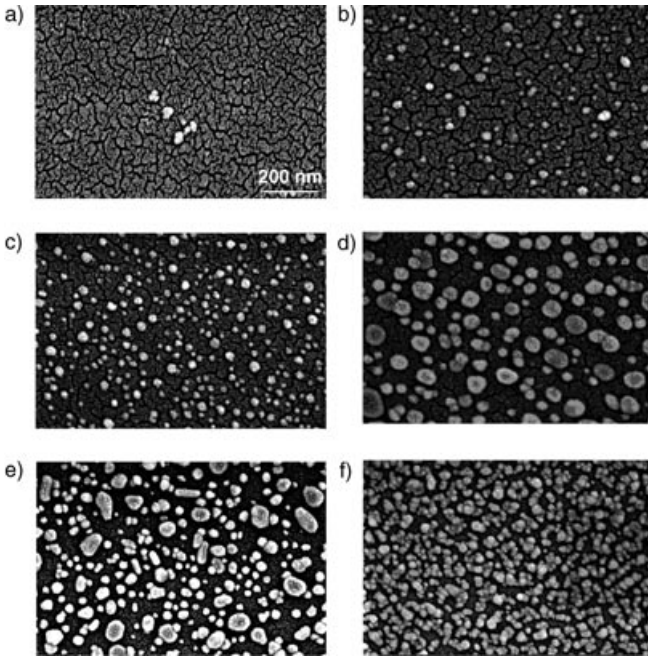

Figure 4. SEM images of enlarged Au particles generated on a Au nanoparticle/3-aminopropylsiloxane interface on a glass support using $AuCl_4^-$ (1.8×10^{-4} M), CTAB (7.4×10^{-2} M), and variable concentrations of NADH: a) 14×10^{-5} M; b) 27×10^{-5} M; c) 41×10^{-5} M; d) 54×10^{-5} M; e) 61×10^{-5} M; f) 1.36×10^{-3} M. All images are on the same scale as indicated in a). All surfaces were coated with a Au/Pt layer (7–8 nm) to enhance the conductivity of the supports.

consistent with the absorbance features of the respective interface shown in Figure 3, curves b, c, e, and i. At high concentrations of NADH (Figures 4e,f), high surface coverages of the enlarged Au particles are observed. Interestingly, the enlarged particles are of smaller dimensions, $\approx 20 \pm 5$ nm, yet the particles touch one another to form 2D Au particle aggregates. This observation is consistent with the observation of an interparticle-coupled plasmon absorbance band for the aggregated nanoparticles on the surface at high concentrations of NADH (see Figure 3, curves k and n, respectively).

The analysis of surface-enlarged Au particles by SEM provides important information on the growth mechanism of the particles in the presence of the $AuCl_4^-$/NADH system: 1) At low concentrations of NADH, the probability of initiating the catalytic enlargement of the Au NP seeds is low. Once the Au NP seeds are activated, they grow effectively. This explains why at low NADH concentrations the surface coverage of the enlarged particles is low but the particles reach dimensions of 30 ± 20 nm. 2) At high concentrations of NADH, the probability of activating the growth of the Au NPs increases. This facilitates the parallel growth of numerous activated seeds which leads to smaller particles (20 ± 5 nm) with a high surface coverage.

Subsequently, the growth of the Au NP seeds by the NADH/$AuCl_4^-$ system was applied to analyze the substrate coupled to a NAD^+-dependent biocatalyzed process. As the growth of the Au NP seeds proceeds in CTAB-rich acidic medium (pH 4.0) we were forced to compartmentalize the analytical assay to prevent direct contact between the enzyme-active solutions and the Au NP growth systems. Figures 5 and 6 depict the analysis of lactate in the presence of the NAD^+-dependent lactate dehydrogenase (LDH) by using the catalytic growth of the Au NP seeds as a readout method. In one compartment, the LDH-mediated reduction of NAD^+ by different concentrations of lactate was allowed to proceed for a fixed reaction time of 30 mins. The resulting biocatalytic mixture that included the LDH-generated NADH was then introduced into the second compartment, which contained the Au NP seeds in the growth solution (Figure 5). In an alternative procedure, the biocatalytic mixture was added to the Au NP/aminosiloxane-functionalized glass surfaces in the presence of $AuCl_4^-$ (Figure 6).

The spectral changes of the Au NP growth solution upon addition of the LDH-generated NADH in the presence of different concentrations of lactate are shown in Figure 5. As the concentration of lactate increases, the concentration of the generated NADH increases. At low concentrations of lactate, the amount of NADH generated is insufficient to reduce all the $AuCl_4^-$ species to the Au^I species and this leads to a residual absorbance of $AuCl_4^-$ at $\lambda = 392$ nm (Figure 5, curves a–c). At concentrations of lactate higher than 0.45 mM, the generated NADH reduces all the $AuCl_4^-$ species to Au^I, and the seeds are effectively enlarged (curves d–g). Figure 5, inset, shows the variation of the absorbance at $\lambda = 524$ nm with different concentrations of lactate. Figure 6, curves a–h, show the bands that correspond to the enlarged particles on the surface (plasmons) that formed after 60 mins by NADH generated biocatalytically. As the concentration of lactate increases, the plasmon absorbance band increases in intensity and is shifted to longer wavelengths. Thus, at higher concentrations of lactate, more Au NP seeds are activated towards the enlargement process and the resulting particles are larger in dimension.

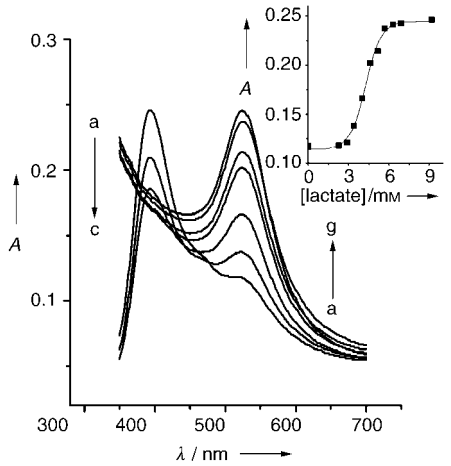

Figure 5. Variation in the absorbance spectra of the growth solution (1.4×10^{-10} M in Au NP seeds) upon the addition of NADH (generated biocatalytically) and variable concentrations of lactate: a) 2.3×10^{-3} M; b) 3.4×10^{-3} M; c) 4.0×10^{-3} M; d) 4.6×10^{-3} M; e) 5.2×10^{-3} M; f) 5.7×10^{-3} M; g) 9.2×10^{-3} M. Inset: Variations in the absorbance of the growth solution as a function of the concentration of lactate in the biocatalysis compartment.

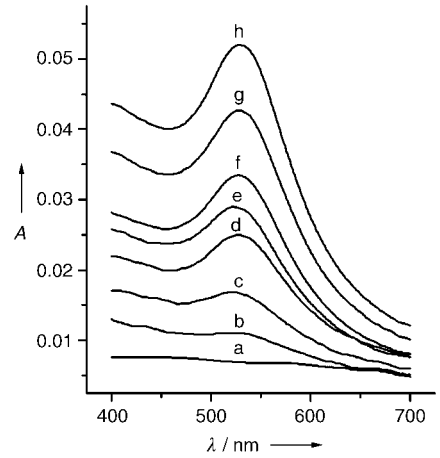

Figure 6. Variation in the absorbance spectra of the Au NP/3-aminopropylsiloxane-functionalized glass slides upon treatment with the growth solution, NADH (generated biocatalytically), and variable concentrations of lactate: a) 0 M; b) 2.9×10^{-3} M; c) 3.6×10^{-3} M; d) 5.1×10^{-3} M; e) 5.8×10^{-3} M; f) 6.6×10^{-3} M; g) 7.3×10^{-3} M; h) 9.8×10^{-3} M.

In conclusion, the present study has demonstrated 1) the enlargement of Au nanoparticles mediated by NADH and 2) an optical readout method based on the absorbance of Au particle-plasmons to monitor biocatalyzed transformations.

Experimental Section

Au NPs (13 ± 2 nm) stabilized with citrate,[17] and Au NPs (3.5 ± 0.5 nm) prepared with $NaBH_4$ and stabilized with citrate[18] were

prepared according to the literature. The concentration of the Au NPs (13 ± 2 nm) was determined from the absorbance value and the appropriate extinction coefficient at $\lambda = 519$ nm. The solution of the Au NPs was used within 2–5 h after preparation. Growth solutions consisted of $HAuCl_4$ (1.8×10^{-4}), CTAB (7.4×10^{-2} M), and different concentrations of NAD(P)H. For the catalytic growth of the gold nanoparticles, Au NPs (1×10^{-10} M in 13 ± 1-nm particles) were added to the growth solution, and the absorbance spectra were recorded after 30 mins at 30 °C. Glass slides were functionalized with 3-aminopropyl triethoxysilane as described previously[15] and modified accordingly with the citrate-stabilized Au NPs (3.5 ± 0.5 nm). The Au NP-modified glass slides were soaked in the growth solution for 1 h at 30 °C. The absorbance spectra of the resulting modified slides were recorded in water. The LDH-mediated oxidation of lactate in the presence of NAD^+, monitored by the enlargement of the Au NPs (as optical labels), was performed in two steps: 1) A solution of Tris buffer (50 mM; pH 9.0) that contained NAD^+ (1×10^{-3} M), LDH (0.2 mg mL^{-1}), and different concentrations of lactate was allowed to react for 30 mins at 30 °C. 2) A 200-μL aliquot of this mixture was then added to the growth solution (2.5 mL; pH 1.8). Au NPs (1.4×10^{-10} M in 13 ± 1-nm particles) or the Au NP-functionalized slides were then added as seeds to the growth solution. The absorbance spectra of the solutions or of the Au NP-functionalized slides, were then recorded after 30 mins at 30 °C.

Received: May 10, 2004 [Z460608]

Keywords: biosensors · cofactors · enzymes · gold · nanostructures

[1] a) C. M. Niemeyer, *Angew. Chem.* **2001**, *113*, 4643 – 4644; *Angew. Chem. Int. Ed.* **2001**, *40*, 4128 – 4158; b) E. Katz, I. Willner, J. Wang, *Electroanalysis* **2004**, *16*, 19 – 44; c) E. Katz, A. N. Shipway, I. Willner in *Nanoparticles—From Theory to Applications* (Ed.: G. Schmid) Wiley-VCH, Weinheim, **2003**, Chapter 6, pp. 368 – 421.

[2] a) J. Wang, G. D. Liu, A. Merkoci, *J. Am. Chem. Soc.* **2003**, *125*, 3214 – 3215; b) J. Wang, G. D. Liu, Q. Y. Zhu, *Anal. Chem.* **2003**, *75*, 6218 – 6222; c) J. Wang, O. Rincon, R. Polsky, E. Dominguez, *Electrochem. Commun.* **2003**, *5*, 83 – 86; d) J. Wang, R. Polsky, D. K. Xu, *Langmuir* **2001**, *17*, 5739 – 5741.

[3] I. Willner, F. Patolsky, J. Wasserman, *Angew. Chem.* **2001**, *113*, 1913 – 1916; *Angew. Chem. Int. Ed.* **2001**, *40*, 1861 – 1864.

[4] V. Pardo-Yissar, E. Katz, J. Wasserman, I. Willner, *J. Am. Chem. Soc.* **2003**, *125*, 622 – 623.

[5] S. J. Park, T. A. Taton, C. A. Mirkin, *Science* **2002**, *295*, 1503 – 1506.

[6] a) X. C. Zhou, S. J. O'Shea, S. F. Y. Li, *Chem. Commun.* **2000**, 953 – 954; b) F. Patolsky, K. T. Ranjit, A. Lichtenstein, I. Willner, *Chem. Commun.* **2000**, 1025 – 1026; c) I. Willner, F. Patolsky, Y. Weizmann, B. Willner, *Talanta* **2002**, *56*, 847 – 856.

[7] a) X. H. Gao, S. M. Nie, *Trends Biotechnol.* **2003**, *21*, 371 – 373; b) A. P. Alivisatos, *Nat. Biotechnol.* **2004**, *22*, 47 – 52.

[8] a) W. J. Parak, D. Gerion, D. Zanchet, A. S. Woerz, T. Pellegrino, C. Micheel, S. C. Williams, M. Seitz, R. E. Bruehl, Z. Bryant, C. Bustamante, C. R. Bertozzi, A. P. Alivisatos, *Chem. Mater.* **2002**, *14*, 2113 – 2119; b) I. L. Medintz, A. R. Clapp, H. Mattoussi, E. R. Goldman, B. Fisher, J. M. Mauro, *Nat. Mater.* **2003**, *2*, 630 – 638; c) L. Y. Wang, L. Wang, F. Gao, Z. Y. Yu, Z. M. Wu, *Analyst* **2002**, *127*, 977 – 980.

[9] S. O. Obare, R. E. Hollowell, C. J. Murphy, *Langmuir* **2002**, *18*, 10407 – 10410.

[10] J. J. Storhoff, C. A. Mirkin, *Chem. Rev.* **1999**, *99*, 1849 – 1862.

[11] J. W. Liu, Y. Lu, *J. Am. Chem. Soc.* **2003**, *125*, 6642 – 6643.

[12] a) L. G. Lee, G. M. Whitesides, *J. Am. Chem. Soc.* **1985**, *107*, 6999 – 7008; b) I. Willner, D. Mandler, *Enzyme Microb. Technol.* **1989**, *11*, 467 – 483.

[13] a) I. Katakis, E. Dominguez, *Microchim. Acta* **1997**, *126*, 11 – 32; b) A. Bardea, E. Katz, A. F. Bückmann, I. Willner, *J. Am. Chem. Soc.* **1997**, *119*, 9114 – 9119.

[14] J. R. Nikhil, G. Latha, M. J. Catherine, *Langmuir* **2001**, *17*, 6782 – 6786.

[15] A. Doron, E. Katz, I. Willner, *Langmuir* **1995**, *11*, 1313 – 1317.

[16] a) A. N. Shipway, M. Lahav, R. Gabai, I. Willner, *Langmuir* **2000**, *16*, 8789 – 8795; b) M. Quinton, U. Kreibig, *Surf. Sci.* **1986**, *172*, 557 – 577; c) C. G. Blatchord, J. R. Campbell, J. A. Creighton, *Surf. Sci.* **1982**, *120*, 435 – 455; d) C. P. Collier, R. J. Saykally, J. J. Shiang, S. E. Henichs, J. R. Heath, *Science* **1997**, *277*, 1978 – 1981.

[17] K. C. Grabar, R. G. Freeman, M. B. Hommer, M. J. Natan, *Anal. Chem.* **1995**, *67*, 735 – 743.

[18] B. D. Brantley, O. O. Sherine, M. J. Catherine, *Adv. Mater.* **2003**, *15*, 414 – 416.

